LDD Land Degradation & Development

Spatial modelling of gully erosion using Evidential Belief Function, Logistic Regression and a new ensemble EBF–LR algorithm

Journal:	*Land Degradation & Development*
Manuscript ID	LDD-18-0480.R3
Wiley - Manuscript type:	Research Article
Date Submitted by the Author:	n/a

Complete List of Authors:	Arab Ameri, Alireza ; Tarbiat Modares University, Geomorphology Pradhan, Biswajeet; University of Technology Sydney Faculty of Engineering and Information Technology, School of Systems, Management and Leadership; University Putra Malaysia Rezaei, Khalil ; Kharazmi University, Faculty of Earth Sciences Yamani, Mojtaba ; University of Tehran, Department of Geomorphology, Pourghasemi, Hamid Reza; Shiraz University, Department of Natural Resources and Environmental Engineering, College of Agriculture, Lombardo, Luigi ; Tübingen University, Department of Geosciences,

Keywords:	Gully erosion, LR, EBF, Ensemble method, GIS

Spatial modelling of gully erosion using Evidential Belief Function, Logistic Regression and a new ensemble EBF–LR algorithm

Short title: Spatial modelling of gully erosion

Alireza Arabameri[1], Biswajeet Pradhan[2,3*], Khalil Rezaei[4], Mojtaba Yamani[5], Hamid Reza Pourghasemi[6], Luigi Lombardo[7]

[1]Department of Geomorphology, Tarbiat Modares University, Tehran, Iran

[2]Centre for Advanced Modelling and Geospatial Information Systems (CAMGIS), Faculty of Engineering and IT, University of Technology Sydney, 2007 NSW, Sydney, Australia

[3]Department of Energy and Mineral Resources Engineering, Choongmu-gwan, ejong University, 209 Neungdong-ro Gwangjin-gu, Seoul, 05006, Republic of Korea

[4]Faculty of Earth Sciences, Kharazmi University, Tehran, Iran.

[5]Department of Geomorphology, Tehran University, Tehran, Iran

[6]Department of Natural Resources and Environmental Engineering, College of Agriculture, Shiraz University, Shiraz, Iran

[7]Department of Geosciences, Tübingen University, Tübingen, Germany

*Email: biswajeet24@gmail.com or Biswajeet.Pradhan@uts.edu.au (corresponding author)

Abstract

This study aims to assess gully erosion sensitivity and delineate gully erosion-prone areas in Toroud Watershed, Semnan Province, Iran. Two different methods, namely, logistic regression and evidential belief function, were evaluated, and a new ensemble method was proposed using the combination of both methods. We initially created a gully erosion inventory map using different resources, including early reports, Google Earth images and Global Positioning Systems (GPS)-aided field surveys. We subsequently split this information randomly and selected 70% (90) of the gullies for calibration and 30% (38) for validation. The method was constructed using a combination of morphometric and thematic predictors that include 16 conditioning parameters. We also assessed the following: i) potential multicollinearity issues using tolerance (TOL) and variance inflation factor indices and ii) covariate effects using LR coefficients and EBF class weights. Results show that land use/land cover, lithology and distance to roads dominate the method with the greatest effect on gully occurrences. We produced three sensitivity maps and evaluated their predictive power through area under the curve (AUC) and seed cell area index (SCAI) analyses. AUC results revealed that the ensemble method presented a considerably higher performance (AUC = 0.909) than the individual LR (0.802) and EBF (0.821) methods. Similarly, SCAI displayed a constant decrease from the ensemble to single methods. The resulted gully erosion susceptibility map could be used by decision-makers and local managers for soil conservation, and for minimizing damages in development activities including construction of infrastructures such as roads and the route of gas and electricity transmission lines.

Keywords: Gully erosion; Logistic Regression; Evidential Belief Function; Ensemble method; GIS; Iran

Introduction

Water-related soil erosion is one of the most important natural hazards in arid and semi-arid regions. Apart from the land degradation, loss of soil resources, reduction of soil fertility, desertification and destruction of human infrastructure (on site impacts), with the deposition of materials in the canals and downstream slopes, impact on surface water resources and quality, and also impose economic and ecological costs to societies and therefore has a negative impact on their sustainability development (off-site impacts) (Ayele et al., 2016). Global estimates show that approximately 6 million hectares of arable land lose their fertility annually due to soil erosion (Worker, 2004). Iran ranks second worldwide in terms of the volume of soil erosion (Najafi, 2005). The annual amount of soil losses in Iran is 2 to 2.5 billion tons, which is equivalent to 8% of the global soil erosion (Najafi, 2005). This amount is significant, considering that Iran's share of land area is 1.1% of the world's land area. Conditions are extremely alarming that in the draft law on soil conservation and water management, more than half the area of Iran (88 million hectares) is declared in a critical state of erosion per hectare (Najafi, 2005). Gully erosion is the main destructive type of water-induced soil erosion worldwide (Pourghasemi et al., 2017; Rahmati et al., 2017). According to various definitions, a gully is a deep channel with steep slope edges caused by soil erosion and has a cross section that is greater than 0.304 m (FAO, 1965; Wang et al., 2016). The gully erosion, as a degradation process, with the destruction of surface and subsoil horizons leads to the massive deformation of the land surface and often causes extreme land degradation. Development of gullies is considered as a catalytic agent of destruction of agricultural land, residential areas, and infrastructures. Therefore, this phenomenon impose extensive damages to humankind (Mekonnen et al., 2017; Pulley et al., 2018).

These results have driven numerous investigations over the last decades, with the aim to develop methods for evaluating gully erosion processes and sensitivity mapping (Shellberg et al., 2016; Rahmati et al., 2017). The latter is a prerequisite for decision makers and land use planners. Geographical Information Systems (GIS) is considered a basic analysis tool for gully erosion sensitivity mapping (GESM) because it effectively manipulates spatial data (McCloskey et al., 2016). Moreover, recent advancement in remote sensing and modelling techniques contribute to significant improvements in GESM (Shellberg et al., 2016). Gully erosion is a compound of different physiographic factors (Dube et al., 2014) that interplay at small and large scales. Therefore, the community has focused its efforts on GIS-based techniques for GESM, including weights-of-evidence (WoE; Rahmati et al., 2016), frequency ratio (FR; Conforti et al., 2011; Umer et al., 2014), logistic regression (LR; Conoscenti et al., 2014), information amount (Conforti et al., 2011), the analytical hierarchy process (AHP; Zakerinejad and Maerker, 2014), multivariate adaptive regression splines (MARS: Gómez-Gutiérrez et al., 2015), artificial neural network (ANN; Rahmati et al., 2017), support vector machine (SVM; Pourghasemi et al., 2017), classification and regression tree (CART; Marker et al., 2011), random forest (RF; Kuhnert et al., 2010), and ensemble of ANN- SVM and maximum entropy (ME), data mining methods (Pourghasemi et al., 2017) .

Generally, statistical methods can obtain accurate results because they can use different datasets (Yilmaz, 2009). Moreover, they commonly involve a catchment to regional scales for gully erosion studies. Such methods derive functional relations between gully erosion occurrences and a set of conditioning factors. In the present study, two statistical methods, namely, evidential belief function (EBF) and LR methods, were applied. Literature review showed that LR and EBF methods have been successfully used for landslide assessment (Pourghasemi et al., 2013; Pham et al., 2016; Wang et al., 2016; Althuwaynee et al., 2012; Bui et al., 2017; Chen et al., 2017). Additionally, machine learning approaches are commonly used in the literature (Oh and Pradhan, 2011; Bui et al., 2012; Althuwaynee et al., 2014; Tehrany et al., 2015).

In compared to other statistical approaches, LR methods allow selecting the variables step by step with the least amount of contingent error rates for the spatiotemporal prediction of the future events outside the training area (Brenning, 2005). LR can include independent variables of categorical or continuous nature (Brenning, 2005). It characterises the type of relationship between gully erosion occurrence and conditioning factors, which can be positive or negative (Lee, 2005). Meanwhile, EBF methods compute the correlation between gully erosion and conditioning factors.

On the basis of the literature review, despite the high capability of the EBF and LR methods in hazard mapping, no comprehensive study on the combination of these methods for GESM exists. The main purpose of this research is to apply an ensemble bivariate (EBF) and multivariate (LR) models as a new approach in Toroud Watershed to identify the risk areas of gully erosion. The results would contribute to the sustainable development in this area and minimise soil and economic losses.

Material and methods

Study area

The Toroud Watershed is covering about 228.85 km^2, lies between the latitudes of 35°18′15″N and 35°33′33″N, and the longitudes of 54°56′33″N and 55°09′02″N in northeastern of Semnan Province, Iran. (Fig. 1). The geomorphology of the study area is controlled by geological, hydrological and structural setting. The northern, western, and eastern sectors of the watershed are located on the cones. Slopes in this region have convex profiles and are often highly dissected by V-shaped valleys. On the other hand, the central, southern, southeastern and southwestern sectors are located on the gentle slopes which are characterized by flat and concave profiles. The average value of elevation and slope in Toroud watershed are 799.5 m and 1.52° respectively. According to the climatic classification in Iran (IDWRM, 2013), the study area has an arid climate (average annual rainfall of 43.8 mm), and rainfall in this area varies from 33.17 mm to 93.83 mm constituting 80% of the rainfall which mainly falls in December and January (IRIMO, 2014). The average annual temperature of the study area is 23.4, varying from 50 degrees in summer to -5 degrees in winter. The study area is mainly covered with deserts and poor pasture. Its lithology is mainly composed of Qft2 (low-level piedmont fan and valley terrace deposits), Qft1 (high-level piedmont fan and valley terrace deposits), PlQc (fluvial conglomerate, piedmont conglomerate and sandstone), Qsf (salt flat) and Murm (light - red to brown marl and gypsiferous marl with sandstone intercalations) (GSI, 1997).

The study area is characterized by poorly evolved soils (Entisols and Aridisol; USDA, 2006). Because of the high concentration of gullies is near roads and agricultural lands, therefore the development of gullies causes massive economic damage to the inhabitants. The study area is selected because of two main reasons: 1) a highway is crossing across this region connecting between the two major provinces of Iran (Isfahan and Khorasan Razavi); 2) the area is highly susceptible to gully erosion due to complex geological formations with the presence of gypsum and salt leading to high evaporation.

Fig. 1 Study area.

Methodology

As shown in Fig. 2, this study is conducted in four stages as follows: (1) preparation of data (Meyer and Martinez-Casasnovas, 1999), (2) application of EBF method and determination of the relationship between gully erosion occurrences and conditioning factors (Al Abadi and Al Ali, 2017), (3) utilisation of the LR method and determination of the effect of conditioning factors (Martinez-Casasnovas et al. 2004), (4) GESM of the study area using individual and combined methods and (5) evaluation of the capability and robustness of the combined method in comparison with the individual EBF and LR methods in terms of receiver operating characteristic (ROC)–area under the curve (AUC) and seed cell area index (SCAI) (Luca et al., 2011).

Fig. 2 Flowchart of the methodology used.

Preparation of dependent and independent variables

Gully erosion inventory map (dependent variable)

The geomorphological community has widely used the hypothesis that events in the past are important for understanding the future (Cama et al., 2017) by using statistical methods and predict various phenomena. This assumption postulates that unless significant environmental changes occur, we can investigate previous events, derive functional relations with respect to a given set of covariates and predict potential future occurrences. The gully erosion literature has also used this hypothesis to study the sensitivity of a given area (Pourghasemi et al., 2017). However, for GESM, the primary requirement includes the data collection or inventory that represents the dependent variable of any predictive method (Pourghasemi et al., 2017).

In the present work, early reports, Google Earth images (dated 22/05/2017) and comprehensive field surveys were used to determine the locations of gully erosion and construct an accurate gully erosion inventory map. A total of 128 gullies in the study area were digitised (Fig. 1). Out of the 128 gully erosion occurrences, 90 cases (70%) were randomly selected to calibrate our methods, and the remaining 38 gullies were used for validation (Cama et al., 2017). Some samples of gullies are shown in Fig. 3.

Fig. 3 Field photographs showing identified gullies in the study area.

Gully erosion conditioning factors (independent variables)

The selection of suitable gully erosion conditioning factors (independent variables) is a main step in the modelling of phenomena, such as gully erosion (Rahmati et al., 2017).

Sixteen geo-environmental parameters were selected on the basis of the relevant literature (Rahmati et al., 2017) and the opinions of academics and natural resources experts. Out of these 16 factors, the geomorphometric ones were derived from a DEM with horizontal resolution of 30 m using the ASTER GDEM elevation data together with ArcGIS 10.5 and SAGA-GIS software.

For clarity, we report the manner in which we computed the less common predictors adopted in this study (i.e., stream length (LS), topography wetness index (TWI) and stream power index (SPI)) as follows (Moore et al., 1991):

$$LS = (A_S/22.13)^{0.6} \times (sin\beta/0.0896)^{1.3}, \quad (1)$$

$$TWI = In\ (A_S/\tan\beta), \quad (2)$$

$$SPI = A_S \times tan_\beta. \quad (3)$$

Where A_S is the special area of the basin (m^2/m) and β is slope in degrees.

Landsat 8 OLI images were selected to extract the Normalized Difference Vegetation Index (NDVI) and land use/land cover (LU/LC) (Fig 4a) using ENVI 5.1 software. The NDVI amount was extracted in ArcGIS 10.5 software.

The lithological unit map (Fig 4b) was obtained from the geological map in 1:100,000-scale (GSI, 1997) and were classified into eight classes on the basis of their lithological characteristics and prior knowledge of their influence on gully erosion occurrence. Table 1 shows the lithological characteristics of Toroud Watershed. A soil type map (Fig 4c) was obtained from the Semnan Agricultural and Natural Resources Research Centre and classified into three classes.

Distance to roads (Fig 4d) was calculated from the topographic map with a scale of 1:50,000. The mean annual rainfall layer was prepared in ArcGIS10.5 environment based on 30 years (1984–2014) of precipitation data of the Toroud, Razveh, Moalleman and Hosseinan Stations from the Iran Meteorological Organisation (IRIMO, 2014).

The classes of each gully erosion conditioning factor are shown in Table 2. The pixel size of all layers is the same with that of the digital elevation method (Dube et al., 2014).

Fig. 4 Some examples of gully erosion conditioning factors, a) LU/LC, b) lithology, c) soil type, and d) distance to road.

Table 1 Description of geological units in the study area.

Table 2 Overview of factors used for GESM.

Multicollinearity analysis of gully erosion conditioning factors

When applying any linear statistical method, the multicollinearity of data may hinder the reliability and interpretation of results (Pradhan and Seeni, 2017, 2018; Pradhan et al., 2017). Multicollinearity is defined as the linear dependency that links two or more independent variables in a dataset. Thus, multicollinearity must be checked even for gully erosion sensitivity methods. Several approaches may be adopted to assess multicollinearity. For example, the least absolute shrinkage and selection operator (Camilo et al., 2017) is popularly used to penalise the number of covariates in each method, thereby removing the redundant information carried by collinear predictors. Alternatively, an example can be found in the literature where the variance inflation factor (VIF) is used to recognise the presence of multicollinearity in data (Cama et al., 2017). Here, we opted for VIF, which is the reciprocal of TOL, and calculated as $1 - R^2$, where R^2 is obtained by regressing each variable with respect to the remaining variables in the multivariate regression (Holloway et al., 2017). A TOL ≤ 0.1 or a VIF ≥ 10 indicates serious multicollinearity (Guo-Liang et al., 2017).

LR method

LR is a multivariate statistical method that corresponds to the generalised linear method (GLM) when the distribution to be fitted corresponds to Bernoulli distribution (Hemasinghe et al., 2018). This distribution describes the probabilities of a binary outcome; thus, it is extremely convenient for predicting the presence or absence of gully erosion. LR can derive multivariate relationships between gullies and a set of predictors, assuming linearity between the target and explanatory variables, the latter being continuous and categorical in nature (Lee, 2005). These relationships can be used in an additive equation to produce the probability of gully occurrence, thereby generating GESMs (Zhou et al., 2018). GLMs, particularly LR, are quantitative methods that determine the influence of each independent variable through the coefficients and anti-logarithm of the coefficients (Lee and Sambath, 2006), which offers geomorphologists a chance to infer which environmental properties may dominate the rise of gully erosion and perform remediation to mitigate such phenomenon. The LR is expressed as follows:

$$P = \frac{1}{1+e^{-z}} \qquad (5)$$

where P is the possibility of gully erosion occurrence, denoted by 0 to 1; and Z denotes the gully erosion conditioning parameters and presumed as a linear composition of the conditioning factors, X_i (i = 1, 2, …, n), as shown as follows:

$$Z = Log\ it\ (P) = Ln\ \frac{p}{1-p} = C_0 + C_1 X_1 + \cdots, + C_n X_n, \qquad (6)$$

where C_0 is the constant coefficient of the method; and X_1, X_2, …, X_n are the coefficients of independent variables C_1, C_2, C_{n}, respectively.

EBF

EBF methods have been successfully used as a data-based approach for potential assessment of mineral deposits and landslide and groundwater sensitivity mapping (Mogaji et al. 2014). Data-driven EBF methods can compute the weight of each class of conditioning factors using the relationship between classes and phenomenon occurrence (Wang et al., 2016). This method has four functions, including belief (Bel), disbelief (Dis), uncertainty (Unc) and plausibility (Pls; Mogaji et al. 2014). These functions are calculated as follows (Park et al., 2011):

$$(\mathrm{Bel}) = \left[\frac{\left[\lambda(\mathrm{T_p})_{\mathrm{Aij}}\right]}{\Sigma\left[\lambda(\mathrm{T_p})_{\mathrm{Aij}}\right]}\right], \quad (7)$$

$$\left[\lambda(\mathrm{T_p})_{\mathrm{Aij}}\right] = \left[\frac{\mathrm{N}(\mathrm{F}\cap\mathrm{A_{ij}})}{\mathrm{N}(\mathrm{F})}\right] / \left[(\mathrm{N}(\mathrm{A_{ij}} - \mathrm{N}(\mathrm{F}\cap\mathrm{A_{ij}})))/[\mathrm{N}(\mathrm{P}) - \mathrm{N}(\mathrm{F})]\right] \quad (8)$$

$$(\mathrm{Dis}) = \frac{\left[\lambda(\overline{\mathrm{T}}_\mathrm{p})_{\mathrm{Aij}}\right]}{\Sigma\left[\lambda(\overline{\mathrm{T}}_\mathrm{p})_{\mathrm{Aij}}\right]}, \quad (9)$$

$$\left[\lambda(\overline{\mathrm{T}}_\mathrm{p})_{\mathrm{Aij}}\right] = \left[\frac{\mathrm{N}(\mathrm{F}\cap\mathrm{A_{ij}})}{\mathrm{N}(\mathrm{F})}\right] / [(\mathrm{N}(\mathrm{P}) - \mathrm{N}(\mathrm{F}) - \mathrm{N}(\mathrm{A_{ij}}) + \mathrm{N}(\mathrm{F}\cap\mathrm{A_{ij}})/\mathrm{N}(\mathrm{P}) - \mathrm{N}(\mathrm{F})], \quad (10)$$

$$(\mathrm{Unc}) = [1 - (Bel) - (Dis)], \quad (11)$$

$$(Pls) = [1 - (Dis)], \quad (12)$$

where $\mathrm{N}(\mathrm{F}\cap\mathrm{A_{ij}})$ is the aggregation of gullies occurring in $\mathrm{A_{ij}}$, $\mathrm{N}(\mathrm{F})$ is the total aggregation of the entire gullies in the study area, $\mathrm{N}(\mathrm{A_{ij}})$ is the aggregation of pixels in $\mathrm{A_{ij}}$ and $\mathrm{N}(\mathrm{P})$ is the aggregation of pixels in the entire study area.

Validation of GESMs

A suitable validation is necessary to produce a reliable GESM for any area (Rahmati et al., 2016). Various validation strategies have been introduced in the literature, among which the ROC curve and its integral (known as AUC) have been widely adopted in the geomorphological community (Pourghasemi et al., 2017) together with Success or prediction rate curve (Frattini et al., 2010), and cell area index (Süzen and Doyuran, 2004).

In this study, we combined AUC and SCAI to provide a comprehensive assessment of the validation performance (Hong et al., 2018; Thai Pham et al., 2018; Lee et al., 2018; Pourghasemi and Rahmati, 2018).

AUC is one of the most useful and efficient methods for predicting and determining the accuracy of models (Gómez-Gutiérrez et al., 2015). In fact, this curve is considered a graphical representation of the true prediction of occurrence and non-occurrence of a phenomenon (Dube et al., 2014). AUC represents the predictive amount of the system by describing its capability to estimate the occurrence (the presence of gully) and non-occurrence (the absence of gully) of events accurately. If a method cannot estimate the occurrence of gullies better than the probable or random point, then the AUC is 0.5 and therefore the least accurate; if the AUC is equal to 1, then the method is the most accurate. AUC values can be classified as follows: 0.5–0.6, poor; >0.6–0.7, average; >0.7–0.8, good; >0.8–0.9, very good; and >0.9–1, excellent (Yesilnacar, 2005). The SCAI validation technique was proposed by Suzen and Doyuran (2004). SCAI is calculated by dividing the percentage of pixels of the specific gully erosion sensitivity class by the percentage of the pixels of existing gullies in the specific gully sensitivity zone. SCAI shows the density of gullies among the gully sensitivity zones (Pawluszek and Borkowski, 2017). In the SCAI indicator, the high and very high susceptibility classes have very small SCAI values, and low and very low susceptibility classes have higher SCAI values (Suzen and Doyuran, 2004).

Results

Multicollinearity test

Before applying the EBF and LR methods, we checked for potential linear dependencies between the pairs of covariates to avoid multicollinearity among variables. The values of TOL and VIF of the 16 conditioning factors were calculated to detect multicollinearity (Table 3). From Table 3, the maximum VIF and minimum TOL were 3.452 and 0.290, respectively. The results indicated that no multicollinearity existed between the conditioning factors.

LR method

In this study, we calculated the regression coefficients of the gully erosion conditioning factors using IDRISI software. The coefficients of the gully erosion conditioning factors using the LR method are shown in Fig. 5. According to LR results, parameters of LU/LC, lithology, distance to road and soil type with scores 0.692, 0.492, 0.385, and 0.355

respectively, have had the greatest effect on the gully erosion. This results are in line with the findings of (Conoscenti et al. 2014). On the contrary, factors of slope aspect, profile curvature, TWI, and drainage density with scores -0.098, -0.0541, -0.054, and -0.026 respectively, have had little impact on the gully erosion. Rest of the parameters such as slope degree, plan curvature, SPI, NDVI, rainfall, distance to stream, convergence index and LS are ranked from fifth to twelfth.

The *z* value is computed as follows:

$$\begin{aligned} Z = -11.7494 &+ (-0.098 \times slope\ aspect) + (0.492 \times lithology) \\ &+ (0.086 \times slope\ degree) + (0.082 + plan\ curvature) \\ &+ (0.01 \times distance\ to\ stream) + (0.043 \times NDVI) + (0.044 \times SPI) \\ &+ (-0.054 \times TWI) + (-0.024 \times LS) + (0.355 \times soil\ type) \\ &+ (-0.026 \times drainage\ density) + (-0.013 \times convergence\ index) \\ &+ (0.693 \times land\ use) + (-0.054 \times profile\ curvature) \\ &+ (0.022 \times rainfall) + (0.385 \times distance\ to\ road). \quad (13) \end{aligned}$$

According to the *z* value, the *P* values were computed using Eq. 5. The P values varied from 0.0032 to 0.074. The subsequent sensitivity amounts were classified into five classes (Fig. 6a) according to the natural breaks method (Guo-Liang et al., 2017). The resulting map indicated that the low class had the largest area (30.85%), followed by the moderate (18.18%), very low (17.56%), high (17.26%) and very high (16.12%) classes. In addition, the largest percentage (47.15%) of the total gullies fell in the very high sensitivity zones, followed by the moderate (27.15%), high (13.11%), low (11.65%) and very low (0.917%) zones (Table 5).

Fig. 5 Coefficients of the conditioning factors in the LR model.

Table 3 Multicollinearity test among conditioning factors.

EBF method

The results of the EBF method are shown in Table 4. The correlation rate between the conditioning factors and the gully erosion occurrence is related on the Bel amounts. The absence of Bel in each class indicates no contribution to gully erosion (Pradhan et al., 2014; Zeinivand and Ghorbani Nejad, 2018). As shown in Table. 4, the slope degree in the class of <1° has the most Bel amount (0.306). This result indicates the utmost effect on gully erosion occurrences. The slope aspect suggests that the SE and F classes have the largest Bel amounts (0.218 and 0.204, respectively); therefore, gully erosion in these classes is high, which is consistent with the findings of Rahmati et al. (2016). On the basis of the profile curvature, the largest degree of belief amounts (0.227) is related to the class of −0.001 to −0.0005.

Table. 4 Spatial relationship between gully erosion occurrence and conditioning factors using EBF model.

In the case of plane curvature, the results show that flat areas with the largest degree of Bel (0.367) contribute a higher probability of gully erosion than the concave (0.338) and convex (0.293) areas. On the basis of NDVI results, classes of 0.039–0.13 and >0.39 with Bel amounts of 0.639 and 0.363, respectively, have a strong relationship with gully occurrence, whereas the class of >0.13 with Bel amount of 0 has no influence on gully erosion. This result is consistent with that of Gomez-Gutierrez et al. (2009). On the basis of the relationship between gully occurrence and LU/LC among the various land uses, desert areas have the largest Bel amount (0.772) and therefore has the largest gully sensitivity. By contrast, irrigated lands have no correlation with gully erosion because of vegetation cover. These results are similar to those of Conoscenti et al. (2014). In the case of lithology, the results indicated that high levels of piedmont fan and valley terrace deposits (Qft1) with maximum

Bel degrees (0.276) show the upmost sensitivity to gully erosion. For the distances to road and river, an inverse relationship exists between the sensitivity of area to gully erosion and Bel degree. In other words, the amount of Bel decreases with the increase in distance of the factors. This result agrees with that of Shellberg et al. (2016), which suggests that anthropogenic linear features in the landscape, such as roads, contribute to flow concentration and thus contribute to gullies. Moreover, Conoscenti et al. (2014) statistically correlated gullies to a river network, which we investigated in the present study, including drainage density. The Bel amounts for drainage effects show that gully erosion sensitivity is high in the class of 2.19–2.54 km/km^2; particularly, a low density indicates a low Bel amount. The analysis of Bel for the relationship between gully erosion occurrence and TWI shows that the class of −0.84–0.94 with the largest Bel amount (0.284) has a strong correlation with gully erosion. According to the rainfall results, the class of 80–85 mm has the largest amount of Bel (0.410). In the case of SPI, the results indicate that the class of 7,000–11,000 has a high sensitivity to gully erosion, and the class of >11,000 with the lowest Bel amount (0.055) has the weakest correlation with gully occurrence. According to the Bel degree of the LS factor, a direct relationship exists between sensitivity to gully occurrence and Bel degree. Therefore, the probability of gully erosion increases proportionally with LS. The interpretation of the role of soil type in the method indicates that the Entisols/Aridisols class with Bel amount of 0.934 has a strong and positive relationship with gully occurrence. These results indicate that these soils are prone to erosion. On the basis of the convergence index, this parameter exhibits a diverse relationship with gully erosion and with increasing convergence. After the computation of the spatial relationship between gully erosion and conditioning factors, the GESM via the EBF method was constructed using Eq. (14).

$$ESM =$$

$$(slope\ aspect_{Bel}) + (lithology_{Bel}) + (slope\ degree_{Bel}) + (plan\ curvature_{Bel}) +$$

$$(distance\ to\ stream_{Bel}) + (NDVI_{Bel}) + (SPI_{Bel}) + (TWI_{Bel}) + (LS_{Bel}) + (soil\ type_{Bel}) + (drainage\ density_{Bel}) + (convergence\ index_{Bel}) + (land\ use_{Bel}) + (profile\ curvature_{Bel}) + (rainfall_{Bel}) + (distance\ to\ road_{Bel}) \quad (14)$$

The result of the EBF method ranges from 1.850 to 6.750. Then, the resultant GESM was divided into five classes from very low to very high (Fig. 6b; Wang et al., 2016, Arabameri et al., 2017). The results of classification indicate that 19.37% and 20.48% of the study area are in the very low and low sensitivity zones, respectively, and 19.83%, 19.97% and 20.35% fall in the moderate, high and very high sensitivity zones, respectively. Moreover, 49.81% and 27.20% of the total gullies fall in the very high and high sensitivity zones, respectively; whereas moderate, low and very low susceptible zones are 15.16%, 6.25% and 1.56% of the gullies, respectively (Table5).

Fig. 6 GESM using LR, EBF and ensemble models.

Table 5 Area of susceptibility classes and SCAI.

Ensemble method

The combination of models compounds the results of individual methods into a combined method to increase the precision of prediction capability and has therefore received considerable interest from researchers (Guo-Liang et al., 2017). In the present work, LR and EBF methods were combined for the GESM of Toroud Watershed to overcome their individual disadvantages. For this purpose, the coefficients obtained by LR were multiplied by the weight obtained in the EBF method using Eq. 15. Finally, the sensitivity of landscape to gully erosion was computed in ArcGIS10.5 using the Weighted Sum Tools.

$$GESM = (-0.098 \times slope\ aspect_{Bel}) + (0.492 \times lithology_{Bel}) + (0.086 \times slope\ degree_{Bel}) + (0.082 + plan\ curvature_{Bel}) + (0.01 \times distance\ to\ stream_{Bel}) +$$

$$(0.043 \times NDVI_{Bel}) + (0.044 \times SPI_{Bel}) + (-0.054 \times TWI_{Bel}) + (-0.024 \times LS_{Bel}) + (0.355 \times soil\ type_{Bel}) + (-0.026 \times drainage\ density_{Bel}) + (-0.013 \times convergence\ index_{Bel}) + (0.693 \times land\ use_{Bel}) + (-0.054 \times profile\ curvature_{Bel}) + (0.022 \times rainfall_{Bel}) + (0.385 \times distance\ to\ road_{Bel}) \quad (15)$$

The resultant map was classified into five classes similar to the EBF and LR methods (Fig. 7c). The results indicate that from the total area (227.97 km^2) of Toroud Watershed, 19.63% (44.76 km^2) belong to the very low sensitivity class, 20.23% (46.11 km^2) to the low class, 20.14% (45.92 km^2) to the moderate class, 19.70% (44.91 km^2) to the high class and 20.28% (46.24 km^2) to the very high sensitivity class. Generally, from the total gully erosion area (2.72 km^2), 0.82% (0.022 km2) fall in the very low sensitivity class, followed by 3.67% (0.1 km^2), 10.93% (0.293 km^2), 20.68% (0.562 km^2) and 63.87% (1.737 km^2) that fall in the low, moderate, high and very high sensitivity classes, respectively.

Validation of the three methods

The results of validation using the AUC and SCAI methods are shown in Tables 5 and 6. According to the AUC results, the combined method has a higher accuracy of 0.909 (90.09%) than the individual statistical methods (EBF 0.821 (82.1%) and LR 0.802 (80.2%)).

In addition, the amount of SCAI in the three methods gradually decrease from very low to very high sensitivity zones; consequently, the values of SCAI decreased from 12.48, 10.53 and 17.39 in the very low sensitivity class to 0.316, 0.430 and 0.348 in the very high sensitivity class in the LR, EBF and ensemble methods, respectively.

Table 6 AUC values of three models.

Discussion

Due to the shortcomings and limitations of each of the quantitative (data-driven and knowledge-based) methods, scientists proposed and developed ensemble methods in order to overcome their disadvantages and increase their efficiency (Tehrany et al., 2014). In this study, two types of bivariate and multivariate data-driven methods, namely, EBF and LR, and their ensemble were applied to produce GESMs. Given that the results of data-driven methods are obtained from data, the input data should be reliable. In this study, early reports, Google Earth images and comprehensive field surveys by GPS were used to produce the gully erosion inventory, from which all the analyses were performed. Bivariate statistical methods (such as EBF) can perform a quantified prediction of sensitivity using the factor class weighted amounts acquired according to the distribution of events (Tehrany et al., 2013; Guo-liang et al., 2017). The main advantage of EBF is that, unlike other bivariate models, EBF supports a series of mass functions including belief, disbelief, uncertainty, and plausibility. Therefore, the results can adequately show quantitative relationships between gully occurrences and conditioning factors by modeling the degree of uncertainty.

The main disadvantage of EBF method is its incapability to compute the weight of conditioning factors. EBF has been used in various research ranging from landslide sensitivity to groundwater potential mapping (Park et al., 2014; Wang et al., 2016; Zeinivand and Ghorbani Nejad, 2018). Wang et al. (2016) stated that the EBF method with AUC = 80.09 is highly capable of predicting areas prone to landslide. Meanwhile, the main advantage of multivariate methods, such as LR, is its capability to evaluate the relationship between an occurrence and the conditioning factors. Thus, such methods enable the assessment of the significance and the removal of causative factors (Pourghasemi et al., 2013; Guo-liang et al., 2017; Raja et al., 2017).

Pourghasemi et al. (2013) showed that binary LR is highly capable of identifying areas prone to landslide compared with other methods. Raja et al. (2017) stated that LR has a high prediction capability. The results of the LR method indicate that the factors of LU/LC, lithology and distance to road with coefficients of 0.693, 0.492 and 0.385, respectively, have the highest effects on gully occurrence. These results are consistent with those of Belayneh et al. (2014), Conoscenti et al. (2014), Shellberg et al. (2016) and McCloskey et al. (2016). The comparison of the ensemble method with the individual LR and EBF methods shows that the combined method has a higher prediction accuracy than the individual methods.

Conclusion

This study was carried out in order to not only investigate the capability of an ensemble model, EBF-LR, to predict the GESM, but also compare its capability with standalone EBF and LR models. Over the years, researchers and natural resource managers around the world have been working on various types of models to asses GESM. In this research, a new scientific methodology framework is proposed using a combination of bivariate (evidential belief function, EBF) and multivariate (Logistic regression, LR) methods implemented in a geographical information system (GIS) to predict gully erosion-prone areas. For this purpose, 16 gully erosion conditioning factors and 90 gully locations (training dataset) are used for modelling and GESM. Subsequently, 38 gully locations (validation dataset) are used for validation of GESMs. The resultant maps can be used for preventive measures and to reduce possible damages caused by them.

In addition, the importance of all gully erosion conditioning factors was investigated based on all modelling approaches. The result of LR method indicates that factors of LU/LC, lithology and distance to road have the greatest effect on gully occurrence in the study area. The results of validation using AUC and SCAI indicators confirm that the proposed integrated method has a higher accuracy than the individual EBF and LR methods. The results show that the areas with very high susceptibility to gully erosion are mainly distributed in the central part of the study area and gully occurrence are highly predicted near the roads and rivers, flat topography, sparse vegetation and susceptible lithology to erosion. Unfortunately, despite the large dispersion of gullies and the erosion activity in the study area, no measures have been considered to control the growth of gullies and the risk of losses from erosion, and the most destructive type of erosion has not been seriously investigated by authorities. The revitalisation of vegetation, which increases surface roughness, improves soil, increases organic matter and decreases runoff; the management of human activities to prevent and reduce their destructive effects, especially on slopes; and the prevention of grazing in areas sensitive to gully erosion are proposed to reduce the rate of erosion in the study area.

Due to the higher accuracy of the GESM using a combined approach, planners and decision-makers can use it to carry out developmental projects such as road construction and electricity and gas transmission lines in order to prevent possible damages.

Conflict of Interest

Authors declare that there is no conflict of interest in regarding the publication of this paper.

Acknowledgements

Thanks to four anonymous reviewers and Editorial comments by Professor C. J. Barrow and Professor Marques, María Jose for their valuable comments, which helped us to improve the quality of the manuscript.

Funding

This research is supported by the UTS under grant numbers 321740.2232335 and 321740.2232357.

References

Arabameri, A.R., Pourghasemi, H.R., & Yamani, M. (2017). Applying different scenarios for landslide spatial modeling using computational intelligence methods. *Environmental Earth Sciences*, **76**, 832. DOI: https://doi.org/10.1007/s12665-017-7177-5.

Al-Abadi, A., & Al-Ali, A. (2018). Susceptibility mapping of gully erosion using GIS-based statistical bivariate models: a case study from Ali Al-Gharbi District, Maysan Governorate, southern Iraq. *Environmental Earth Sciences*, **77**, 249. DOI: https://doi.org/10.1007/s12665-018-7434-2.

Althuwaynee, O.F., Pradhan, B., & Lee, S. (2012). Application of an evidential belief function model in landslide susceptibility mapping, *Computers and Geosciences*, **44**, 120-135. DOI: https://doi.org/10.1016/j.cageo.2012.03.003.

Althuwaynee, O.F., Pradhan, B., Park, H.J., & Lee, J.H. (2014). A novel ensemble bivariate statistical evidential belief function with knowledge-based analytical hierarchy process and multivariate statistical logistic regression for landslide susceptibility mapping. *Computers and Geosciences*, **114**, 21-36. DOI: https://doi.org/10.1016/j.catena.2013.10.011

Ayele, G.K., Gessess, A.A., Addisie, M.B., Tilahun, S.A., Tebebu, T.Y., Tenessa, D.B., Langendoen, E.J., Nicholson, C.F., & Steenhuis, T.S. (2016). A biophysical and economic assessment of a community-based rehabilitated gully in the Ethiopian highlands. *Land Degradation & Development*, **27**, 270-280. DOI: https://doi.org/10.1002/ldr.2425.

Belayneh, L., Bantider, A., & Moges, A. (2014). Road construction and gully development in Hadero Tunto-Durgi road project, Southern Ethopia. *Ethiopian Journal of Environmental Studies and Management*, **7**, 720–730. DOI: 10.4314/ejesm.v7i1.3S.

Brenning, A. (2005). Spatial prediction models for landslide hazards: review, comparison and evaluation. *Natural Hazards and Earth System Sciences*, **5**, 853–862. DOI: https://doi.org/10.5194/nhess-5-853-2005.

Bui, D.T., Bui, Q.T., Nguyen, Q.P., Pradhan, B., Nampak, H., & Trinh, P.T. (2017). A hybrid artificial intelligence approach using GIS-based neural-fuzzy inference system and particle swarm optimization for forest fire susceptibility modeling at a tropical area. *Agricultural and Forest Meteorology*, **233**, 32-44. DOI: https://doi.org/10.1016/j.agrformet.2016.11.002

Bui, D.T., Pradhan, B., Lofman, O., Revhaug, I., & Dick, O.B. (2012). Landslide susceptibility mapping at Hoa Binh province (Vietnam) using an adaptive neuro-fuzzy inference system and GIS. *Computers & Geosciences,* **45**, 199-211. DOI: https://doi.org/10.1016/j.cageo.2011.10.031

Cama, M., Lombardo, L., Conoscenti, C., & Rotigliano, E. (2017). Improving transferability strategies for debris flow susceptibility assessment: application to the Saponara and Itala catchments (Messina, Italy). *Geomorphology*, **288**, 52–65. DOI: https://doi.org/10.1016/j.geomorph.2017.03.025

Camilo, D., Lombardo, L., Mai, P., Dou, J., & Huser, R. (2017). Handling high predictor dimensionality in slope-unit-based landslide susceptibility models through LASSO penalized Generalized Linear Model. *Environmental Modelling and Software*, **97**, 145-156. DOI: https://doi.org/10.1016/j.envsoft.2017.08.003

Chen, W., Xie, X., Wang, J., Pradhan, B., Hong, H., Bui, D.T., Duan, Z., & Ma, J. A. (2017). Comparative study of logistic model tree, random forest, and classification and regression tree models for spatial prediction of landslide susceptibility. *Catena*, **151**, 147-160. DOI: https://doi.org/10.1016/j.catena.2016.11.032

Conoscenti, C., Angileri, S., Cappadonia, C., Rotigliano, E., Agnesi, V., & Ma¨rker, M. (2014). Gully erosion susceptibility assessment by means of GIS-based logistic regression: a case of Sicily (Italy). *Geomorphology*, **204 (1)**, 399–411. DOI: https://doi.org/10.1016/j.geomorph.2013.08.021

Conforti, M., Aucelli, P.P., Robustelli, G., & Scarciglia, F. (2011). Geomorphology and GIS analysis for mapping gully erosion susceptibility in the Turbolo stream catchment (Northern Calabria, Italy). *Natural Hazards,* **56 (3)**, 881–898. DOI: https://doi.org/10.1007/s11069-010-9598-2

Dempster, A.P. (1967). Upper and lower probabilities induced by a multivalued mapping. *The Annals of Mathematical Statistics,* **38 (2)**, 325–339.

Frattini, P., Crosta, G.B., & Carrara, A. (2010). Techniques for evaluating the performance of landslide susceptibility models. *Engineering Geology*, **111 (1-4)**, 62–72. DOI: https://doi.org/10.1016/j.enggeo.2009.12.004

Food and Agricultural Organization-FAO, (1965). Soil Erosion by Water, Some Measures for its Control on Cultivated Land. FAO Agricultural, Rome, 81.

Gómez-Gutiérrez, Á., Conoscenti, C., Angileri, S.E., Rotigliano, E., & Schnabel, S. (2015). Using topographical attributes to evaluate gully erosion proneness (susceptibility) in two Mediterranean basins: advantages and limitations. *Natural Hazards*, **79 (1)**, 291–314. DOI: https://doi.org/10.1007/s11069-015-1703-0

Guo-liang, D., Yong-shuang, Z., Javed, I., Zhi-hua, Y, & Xin, Y. (2017). Landslide susceptibility mapping using an integrated model of information value method and logistic regression in the Bailongjiang watershed, Gansu Province, China. *Journal of Mountain Science*, **14(2)**, 249-268. DOI: https://doi.org/10.1007/s11629-016-4126-9

Geology Survey of Iran (GSI). (1997). http://www.gsi.ir/Main/Lang¬¬_en/index.html.

Holloway, J., Rudy, A., Lamoureux, S., & Treitz, P. (2017). Determining the terrain characteristics related to the surface expression of subsurface water pressurization in permafrost landscapes using susceptibility modeling. *The Cryosphere*, **11**, 1403–1415. DOI: https://doi.org/10.5194/tc-11-1403-2017

Hong, H., Liu, J., Tien Bui, D., Pradhan, B., Acharya, T., & Bin Ahmad, B. (2018). Landslide susceptibility mapping using J48 Decision Tree with AdaBoost, Bagging and Rotation Forest ensembles in the Guangchang area (China). *Catena*, **163**, 399-413. DOI: https://doi.org/10.1016/j.catena.2018.01.005

Hemasinghe, H., Rangali, R.S.S., Deshapriya, N.L., Samarakoon, L. (2018). Landslide susceptibility mapping using logistic regression model (a case study in Badulla District, Sri Lanka). *Procedia Engineering*, 212, 1046-1053. DOI: https://doi.org/10.1016/j.proeng.2018.01.135

I.R. of Iran Meteorological Organization. (2014). http://www.mazan daranmet.ir.

Iranian Department of Water Resources Management (IDWRM), 2013. Weather and climate report. http://www.thrw.ir/ (Accessed 25 June 2013).

Lee, S. (2005). Application of logistic regression model and its validation for landslide susceptibility mapping using GIS and remote sensing data. *International Journal of Remote Sensing*, **26**, 1477–1491. DOI: https://doi.org/10.1080/01431160412331331012

Lee, S., & Sambath, T. (2006). Landslide susceptibility mapping in the Damreiromal area,Cambodia using frequency ratio and logistic regression models. *Journal of Environmental Geology*, **50**, 847-855. DOI: https://doi.org/10.1155/2017/3730913

Lee, J., Sameen, M., Pradhan, B., & Park, H.J. (2018). Modeling landslide susceptibility in data-scarce environments using optimized data mining and statistical methods. *Geomorphology*, **303**, 284-298. DOI: https://doi.org/10.1016/j.geomorph.2017.12.007.

Luca, F., Conforti, M., & Robustelli, G. (2011). Comparison of GIS-based gullying susceptibility mapping using bivariate and multivariate statistics: Northern Calabria, South Italy. *Geomorphology,* **134 (3-4)**, 297–308. DOI: https://doi.org/10.1016/j.geomorph.2011.07.006

Martinez-Casasnovas, J.A., RamosM M.C., & Poesen, J. (2004). Assessment of sidewall erosion in large gullies using multi-temporal DEMs and logistic regression analysis. *Geomorphology,* **58 (1-4)**, 305–321. DOI: https://doi.org/10.1016/j.geomorph.2003.08.005

Marker, M., Pelacani, S., & Schro¨der, B. (2011). A functional entity approach to predict soil erosion processes in a small Plio-Pleistocene Mediterranean catchment in Northern Chianti, Italy. *Geomorphology,* **125 (4)**, 530–540. DOI: https://doi.org/10.1016/j.geomorph.2010.10.022

Mekonnen, M., Keesstra, S.D., Baartman, J.E., Stroosnijder, L., & Maroulis, J. (2017). Reducing Sediment Connectivity Throughman-Made and Natural Sediment Sinks in the Minizr Catchment, Northwest Ethiopia. *Land Degradation and Development*, **28 (2)**, 708–717. DOI: https://doi.org/10.1002/ldr.2629

Meyer, A., & Martı´nez-Casasnovas, J.A. (1999). Prediction of existing gully erosion in vineyard parcels of the NE Spain: a logistic modelling approach. *Soil and Tillage Research*, **50 (3-4)**, 319–331. DOI: https://doi.org/10.1016/S0167-1987(99)00020-3

McCloskey, G.L., Wasson, R.J., Boggs, G.S., & Douglas, M. (2016). Timing and causes of gully erosion in the riparian zone of the semi-arid tropical Victoria River, Australia: management implications. *Geomorphology,* **266**, 96–104. DOI: https://doi.org/10.1016/j.geomorph.2016.05.009

Najafi, Q. 2005. Land and agricultural lands in Iran. *Monthly Dehati Magazine*, **24**: 17-24. (in Persian).

Oh, H.J., & Pradhan, B. (2011). Application of a neuro-fuzzy model to landslide-susceptibility mapping for shallow landslides in a tropical hilly area. *Computers & Geosciences*, **37(9)**, 1264-1276. DOI: https://doi.org/10.1016/j.cageo.2010.10.012

Pourghasemi, H.R., Moradi, H.R., & Aghda, S.M.F. (2013). Landslide susceptibility mapping by binary logistic regression, analytical hierarchy process, and statistical index models and assessment of their performances. *Natural Hazards*, **69(1)**, 749-779. DOI: https://doi.org/10.1007/s11069-013-0728-5

Pham, B.T., Pradhan, B., Bui, D.T., Prakash, I., & Dholakia, M.A. (2016). Comparative study of different machine learning methods for landslide susceptibility assessment: a case study of Uttarakhand area (India). Environmental Modelling & Software, **84**, 240-250. DOI: https://doi.org/10.1016/j.envsoft.2016.07.005

Pourghasemi, H.R., Yousefi, S., Kornejady, A., & Cerdà, A. (2017). Performance assessment of individual and ensemble data-mining techniques for gully erosion modeling. *Science of the Total Environment*, **609**, 764–775. DOI: https://doi.org/10.1016/j.scitotenv.2017.07.198

Pourghasemi, H., & Rahmati, O. (2018). Prediction of the landslide susceptibility: Which algorithm, which precision?. *Catena,* **162**, 177-192. DOI: https://doi.org/10.1016/j.catena.2017.11.022

Pradhan, B., & Seeni, M.I. (2018). Manifestation of SVM-Based Rectified Linear Unit (ReLU) Kernel Function in Landslide Modelling. *Space Science and Communication for Sustainability*: 185-195. DOI: https://doi.org/10.1007/978-981-10-6574-3_16

Pradhan, B., Seeni, M.I., & Kalantar, B. (2017). Performance evaluation and sensitivity analysis of expert-based, statistical, machine learning, and hybrid models for producing landslide susceptibility maps. In: Pradhan B. (eds) Laser scanning applications in landslide assessment. *Springer International Publishing*, 193–232. DOI: https://doi.org/10.1007/978-981-10-6574-3_16

Pradhan, B., & Sameen, M.I. (2017). Landslide susceptibility modeling: optimization and factor effect analysis. In: Pradhan B. (eds) Laser Scanning Applications in Landslide Assessment. *Springer International Publishing*, 115–132. DOI: https://doi.org/10.1007/978-3-319-55342-9_6

Pradhan, A.M.S., & Kim, Y.T. (2014). Relative effect method of landslide susceptibility zonation in weathered granite soil: A case study in Deokjeok-ri Creek, South Korea. *Natural Hazards,* **72(2)**, 1189–1217. DOI: https://doi.org/10.1007/s11069-014-1065-z

Pulley, S., Ellery, W.N., Lagesse, J.V., Schlegel, P.K., Mcnamara, S.J.(2018). Gully erosion as a mechanism for wetland formation: An examination of two contrasting landscapes. *Land Degradation and Development*, **29 (6)**, 1756 – 1767. DOI: https://doi.org/10.1002/ldr.2972

Raja, N., Cicek, I., Turkoglu, N., Aydin, O., & Kawasak, A. (2017). Landslide susceptibility mapping of the Sera River Basin using logistic regression model. *Natural Hazards*, **85**, 1323–1346. DOI: https://doi.org/10.1007/s11069-016-2591-7

Rahmati, O., Haghizadeh. A., Pourghasemi, H.R., & Noormohamadi, F. (2016). Gully erosion susceptibility mapping: the role of GIS based bivariate statistical models and their comparison, *Natural Hazards*, **82**, 1231–1258. DOI: https://doi.org/10.1007/s11069-016-2239-7

Rahmati, O., Tahmasebipour, N., Haghizadeh, A., Pourghasemi, H.R. & Feizizadeh, B. (2017). Evaluation of different machine learning models for predicting and mapping the susceptibility of gully erosion, *Geomorphology*, **298**, 118-137. DOI: https://doi.org/10.1016/j.geomorph.2017.09.006

Shafer, G. (1976). *A mathematical theory of evidence*, Princeton University Press, Princeton. DOI: https://doi.org/10.1016/j.ijar.2016.07.009

Shellberg, J.G., Spencer, J., Brooks, A.P., & Pietsch, T.J. (2016). Degradation of the Mitchell River fluvialmegafan by alluvial gully erosion increased by post-European land use change, Queensland, Australia. *Geomorphology,* **266**, 105–120. DOI: https://doi.org/10.1016/j.geomorph.2016.04.021

Süzen, M.L., & Doyuran, V. (2004). A comparison of the GIS based landslide susceptibility assessment methods: multivariate versus bivariate. *Environmental Geology*, **45(5)**, 665–679. DOI: https://doi.org/10.1007/s00254-003-0917-8

Tehrany, M. S., Lee, M. J., Pradhan, B., Jebur, M. N., & Lee, S. (2014). Flood susceptibility mapping using integrated bivariate and multivariate statistical models. *Environmental Earth Sciences*, **72 (10)**, 4001-4015. DOI: https://doi.org/10.1007/s12665-014-3289-3

Tehrany, M. S., Pradhan, B., & Jebur, M. N. (2013). Spatial prediction of flood susceptible areas using rule based decision tree (DT) and a novel ensemble bivariate and multivariate statistical models in GIS. *Journal of Hydrology*, **504**, 69-79. DOI: https://doi.org/10.1016/j.jhydrol.2013.09.034

Tehrany, M.S., Pradhan, B., Mansor, S., & Ahmad, N. (2015). Flood susceptibility assessment using GIS-based support vector machine model with different kernel types. *Catena*, **125**, 91-101. DOI: https://doi.org/10.1016/j.catena.2014.10.017

USDA. (2006). Keys to Soil Taxonomy. USDA (United States Department of Agriculture), Soil Survey Staff, 10th ed. Natural Resources Conservation Service, Washington D.C. 333 pp.

Worker, B., 2004. Evaluation of soil erosion in the Harevge region of Ethiopia using soil loss models, rain simulation and field trials. Thesis for degree Doctor of philosophy, University of Pretoria, Pretoria. URI: http://hdl.handle.net/2263/26929

Wang, Q., Li, W., Wu, Y., Pel, Y., Xing, M., & Yang, D. (2016). A comparative study on the landslide susceptibility mapping using evidential belief function and weights of evidence models, *Journal of Earth System Science*, **125 (3)**, 645–662. DOI: https://doi.org/10.1007/s12040-016-0686-x

Yesilnacar, E.K. (2005). The application of computational intelligence to landslide susceptibility mapping in Turkey. Ph.D Thesis Department of Geomatics the University of Melbourne, 423.

Zakerinejad, R., & Marker, M. (2014). Prediction of Gully erosion susceptibilities using detailed terrain analysis and maximum entropy modeling: a case study in the Mazayejan Plain, Southwest Iran. *Geografia Fisica e Dinamica Quaternaria*, **37 (1)**, 67–76. DOI: http://dx.doi.org/10.4461/GFDQ.2014.37.7

Zeinivand, H., & Ghorbani Nejad, S. (2018). Application of GIS-based data-driven models for groundwater potential mapping in Kuhdasht region of Iran. *Geocarto International*, **33 (6)**, 651-666. DOI: https://doi.org/10.1080/10106049.2017.1289560

Zhou, C., Yin, K., Cao, Y., Ahmed, B., Li, Y., Catani, F., & Pourghasemi, H.R. (2017). Landslide susceptibility modeling applying machine learning methods: A case study from Longju in the Three Gorges Reservoir area, China. *Computers and Geosciences,* **112**, 23–37. DOI: https://doi.org/10.1016/j.cageo.2017.11.019

List of Figures

List of Tables

TABLE 1 Description of geological units in the study area (GSI, 1997)

Class	Lithology	Age	AGE_ERA
Qft2	Low level piedmont fan and valley terrace deposits	Quaternary	CENOZOIC
PlQc	Fluvial conglomerate, Piedmont conglomerate and sandstone.	Pliocene-Quaternary	CENOZOIC
Qft1	High level piedmont fan and valley terrace deposits	Quaternary	CENOZOIC
Murm	Light - red to brown marl and gypsiferous marl with sandstone intercalations	Miocene	CENOZOIC
Mur	Red marl, gypsiferous marl, sandstone and conglomerate (Upper red Fm.)	Miocene	CENOZOIC
Qsf	Salt flat	Quaternary	CENOZOIC
Edav	Dacitic to Andesitic volcanic	Eocene	CENOZOIC
E1c	Pale-red, polygenic conglomerate and sandstone	Paleocene-Eocene	CENOZOIC

TABLE 2 Overview of factors used for Gully Erosion Susceptibility Mapping.

Factor	Range		Classes	Method
	min	max		
Slope	0.00	18.158	1. (<1°), 2- (1-2°), 3. (2-3°), 4. (3-5°), 5. (>5°)	Natural break
Aspect	-1	360	1. Flat (-1°), 2. North (337.5-360°, 0-22.5°), 3. Northeast (22.5- 67.5°), 4. East (67.5-112.5°), 5. Southeast (112.5-157.5°), 6. South (157.5-202.5°), 7. Southwest (202.5-247.5°), 8. West (247.4-292.5°), and 9. Northwest (292.5-337.5°)	Equal interval
Plan curvature	-0.01	0.009	1. Concave (< 0), 2. Flat (0), 3. Convex (> 0)	Natural break
Profile curvature	-0.01	0.013	1. (-0.01 - -0.001), 2. (-0.001- -0.0005), 3. (-0.0005-0.0005), 4. (0.0005- 0.001), 5. (0.001-0.013)	Natural break
LS	0	457.37	1. (<50m), 2. (50-150m), 3. (150-250m), 4. (250-350m), 5. (>350m)	Natural break
NDVI	-0.112	0.403	1. (<0.039), 2. (0.039 - 0.1), 3. (>0.130)	Natural break
TWI	-3.22	6.907	1. (< -0.84), 2. (-0.84 – 0.94), 3. (0.94 – 4), 4. (>4)	Natural break
SPI	0.713	24294	1. (<300), 2. (300 – 1500), 3. (1500 – 3000), 4. (3000 – 7000), 5. (7000 – 11000), 6. (>11000)	Natural break
Drainage density	1.190	3.246	1. (<1.86Km/Km2), 2. (1.86 – 2.19 Km/Km2), 3. (2.19 – 2.54K m/Km2), 4. (> 2.54 Km/Km2)	Natural break
Distance to road	0	13684.7	1. (<500m), 2. (500 – 1000m), 3. (1000 – 1500m), 4. (1500 – 2000m), 5. (>2000m)	Natural break
Distance to river	0	636.39	1. (<100m), 2. (100 - 200m), 3. (200 – 300m), 4. (>300m)	Natural break
LU/LC	-	-	1. (Irrigated lands), 2. (Desert), 3. (Pasture), 4. (salty lands)	Supervised classification
Lithology	-	-	1. (Qft2), 2. (PlQc), 3. (Qft1), 4. (Murm), 5. (Mur), 6. (Qsf), 7. (Edav), 8. (E1c)	Lithological units
Rainfall	73.17	93.70	1. (< 77.60 mm), 2. (77.60 – 81.70mm), 3. (81.70 – 85.41mm), 4. (85.41 – 88.79mm), 5. (>88.79mm)	Natural break
Soil type	-	-	1. (Entisols/Aridisols), 2. (Salty flats), 3. (Rocky lands)	Supervised classification
Convergence	-100	100	1. (< -30), 2. (-30 - -2), 3. (-2 – 30), 4. (> 30)	Natural break

TABLE 3 Multicollinearity test among conditioning factors.

Factors	Multi-collinearity test		Factors	Multi-collinearity test	
	Tolerance	VIF		Tolerance	VIF
Lithology	**0.632**	**1.582**	Plan curvature	**0.773**	**1.294**
LU/LC	**0.483**	**2.070**	NDVI	**0.398**	**2.511**
Soil type	**0.353**	**2.829**	LS	**0.718**	**1.394**
Convergence	**0.784**	**1.275**	Rainfall	**0.723**	**1.382**
Drainage density	**0.290**	**3.452**	Slope degree	**0.583**	**1.716**
Distance to road	**0.296**	**3.382**	SPI	**0.616**	**1.623**
Distance to stream	**0.903**	**1.107**	TWI	**0.818**	**1.222**
Profile curvature	**0.837**	**1.194**	Aspect	**0.918**	**1.089**

TABLE 4 Spatial relationship between gully occurrence and conditioning factors

Factors	Classes	Pixel of domain		Pixel of gullies		EBF			
		N	%	N	%	BEL	DIS	UNC	PLS
Slope (degree)	< 1	114459	45.02	393	55.51	**0.31**	0.16	0.53	0.84
	1 - 2	91337	35.93	226	31.92	**0.22**	0.21	0.56	0.79
	2 - 3	32337	12.72	59	8.33	**0.16**	0.21	0.62	0.79
	3 - 5	12799	5.03	25	3.53	**0.17**	0.21	0.62	0.79
	> 5	3297	1.30	5	0.71	**0.14**	0.20	0.66	0.80
Slope Aspect	F	15826	6.25	66	9.59	**0.20**	0.14	0.66	0.86
	N	9417	3.72	16	2.33	**0.08**	0.15	0.77	0.85
	NE	25783	10.17	49	7.12	**0.09**	0.15	0.76	0.85
	E	46880	18.50	105	15.26	**0.11**	0.15	0.74	0.85
	SE	48387	19.09	216	31.40	**0.22**	0.12	0.66	0.88
	S	36258	14.31	145	21.08	**0.20**	0.13	0.67	0.87
	SW	32005	12.63	62	9.01	**0.09**	0.15	0.75	0.85
	W	20605	8.13	23	3.34	**0.05**	0.15	0.79	0.85
	NW	15135	5.97	21	3.05	**0.07**	0.15	0.78	0.85
Plan Curvature (100/m)	concave	51659	20.32	141	19.92	**0.34**	0.34	0.32	0.66
	flat	148111	58.26	438	61.86	**0.37**	0.31	0.32	0.69
	convex	54458	21.42	129	18.22	**0.29**	0.35	0.35	0.65
Profile Curvature (100/m)	-0.01 - -0.001	7735	3.04	21	2.95	**0.21**	0.20	0.59	0.80
	-0.001- -0.0005	71188	28.00	209	29.35	**0.23**	0.20	0.58	0.80
	-0.0005 - 0.0005	99643	39.19	283	39.75	**0.22**	0.20	0.58	0.80
	0.0005 - 0.001	68560	26.97	187	26.26	**0.21**	0.20	0.59	0.80
	> 0.001	7102	2.79	12	1.69	**0.13**	0.20	0.67	0.80
NDVI	> 0.039	107854	42.52	214	29.85	**0.36**	0.42	0.22	0.58
	0.039 - 0.130	144980	57.16	503	70.15	**0.64**	0.24	0.13	0.76
	>0.130	792	0.31	0	0	**0**	0.34	0.66	0.66
LU/LC	Irrigated lands	2349	0.93	0	0	**0**	0.25	0.75	0.75
	Desert	110530	43.62	502	72.97	**0.77**	0.12	0.11	0.88
	Pasture	138239	54.55	186	27.03	**0.23**	0.39	0.38	0.61
	salty lands	2288	0.90	0	0	**0**	0.25	0.75	0.75
Lithology	Qft2	97841	38.61	237	34.45	**0.13**	0.15	0.72	0.85
	PlQc	37999	15.00	136	19.77	**0.19**	0.13	0.67	0.87
	Qft1	28107	11.09	144	20.93	**0.28**	0.13	0.60	0.87
	Murm	35924	14.18	116	16.86	**0.17**	0.14	0.69	0.86
	Mur	13160	5.19	55	7.99	**0.23**	0.14	0.64	0.86
	Qsf	35824	14.14	0	0	**0**	0.17	0.83	0.83
	Edav	4333	1.71	0	0	**0**	0.14	0.86	0.86
	E1c	218	0.09	0	0	**0**	0.14	0.86	0.86
Distance to road (m)	< 500	23651	9.30	275	38.68	**0.45**	0.11	0.44	0.89
	500 - 1000	19078	7.50	131	18.42	**0.26**	0.15	0.59	0.85
	1000 - 1500	15096	5.94	65	9.14	**0.16**	0.16	0.68	0.84
	1500 - 2000	14317	5.63	31	4.36	**0.08**	0.17	0.75	0.83
	> 2000	182133	71.63	209	29.40	**0.04**	0.41	0.54	0.59
Distance to river (m)	< 100	112480	44.24	322	45.29	**0.27**	0.25	0.49	0.75
	100 - 200	74160	29.17	198	27.85	**0.25**	0.26	0.50	0.74
	200 - 300	48112	18.92	150	21.10	**0.29**	0.24	0.47	0.76
	>300	19523	7.68	41	5.77	**0.20**	0.26	0.55	0.74
Drinage density (km/km2)	< 1.86	29875	11.75	37	5.20	**0.12**	0.27	0.60	0.73
	1.86 - 2.19	94154	37.03	273	38.40	**0.29**	0.25	0.46	0.75
	2.19 - 2.54	76868	30.23	304	42.76	**0.40**	0.21	0.39	0.79
	> 2.54	53378	20.99	97	13.64	**0.18**	0.28	0.54	0.72

Continue

Factors	Classes	Pixel of domain		Pixel of gullies		EBF			
		N	%	N	%	BEL	DIS	UNC	PLS
Rainfall (mm)	< 75	52972	20.84	24	3.37	**0.03**	0.25	0.72	0.75
	75 - 80	38491	15.14	140	19.66	**0.28**	0.19	0.53	0.81
	80 - 85	58041	22.83	314	44.10	**0.41**	0.15	0.44	0.85
	85 - 90	66082	25.99	219	30.76	**0.25**	0.19	0.56	0.81
	> 90	38643	15.20	15	2.11	**0.03**	0.23	0.74	0.77
TWI	< -0.84	38462	15.13	111	15.68	**0.25**	0.25	0.50	0.75
	-0.84 - 0.94	53947	21.22	174	24.58	**0.28**	0.24	0.48	0.76
	0.94 - 4	33355	13.12	87	12.29	**0.23**	0.25	0.52	0.75
	> 4	128465	50.53	336	47.46	**0.23**	0.26	0.51	0.74
SPI	< 300	165290	65.02	428	60.45	**0.15**	0.19	0.66	0.81
	300 - 1500	34236	13.47	106	14.97	**0.18**	0.16	0.66	0.84
	1500 - 3000	29230	11.50	95	13.42	**0.19**	0.16	0.65	0.84
	3000 - 7000	15491	6.09	35	4.94	**0.13**	0.17	0.70	0.83
	7000 - 11000	8927	3.51	43	6.07	**0.28**	0.16	0.56	0.84
	> 11000	1055	0.41	1	0.14	**0.06**	0.16	0.78	0.84
LS (m)	< 50	70459	27.71	161	22.74	**0.16**	0.21	0.63	0.79
	50 - 150	35370	13.91	99	13.98	**0.20**	0.20	0.60	0.80
	150 - 250	46128	18.14	130	18.36	**0.20**	0.20	0.60	0.80
	250 - 350	60273	23.71	179	25.28	**0.21**	0.20	0.59	0.80
	> 350	41999	16.52	139	19.63	**0.23**	0.19	0.57	0.81
Soil type	Entisols/Aridisols	216912	85.60	680	98.84	**0.93**	0.04	0.03	0.96
	Salty flats	372	0.15	0	0	**0**	0.45	0.55	0.55
	Rocky lands	36122	14.25	8	1.16	**0.07**	0.52	0.42	0.48
Cinvergence index (100/m)	< -30	30848	12.13	104	14.69	**0.29**	0.24	0.47	0.76
	-30 - -2	82064	32.28	256	36.16	**0.27**	0.23	0.50	0.77
	-2 - 30	104966	41.29	250	35.31	**0.21**	0.27	0.52	0.73
	> 30	36351	14.30	98	13.84	**0.23**	0.25	0.52	0.75

TABLE 5 Area of susceptibility classes and seed cell area index (SCAI).

Models	Classes	Total area (km^2)		Testing gullies (km^2)		Validation gullies (km^2)		Sum	SCAI
		Area	%	Area	%	Area	%		
LR	Very Low	40.20	17.57	0.03	1.41	0.00	0.00	1.41	**12.49**
	Low	70.62	30.86	0.31	17.58	0.01	0.00	17.58	**1.76**
	Moderate	41.62	18.19	0.40	22.36	0.34	0.09	22.45	**0.81**
	High	39.50	17.26	0.14	7.74	0.22	0.06	7.79	**2.21**
	Very High	36.91	16.13	0.91	50.91	0.38	0.10	51.01	**0.32**
EBF	Very Low	44.11	19.35	0.03	1.83	0.01	0.00	1.84	**10.54**
	Low	46.70	20.48	0.13	7.19	0.04	0.01	7.20	**2.84**
	Moderate	45.22	19.84	0.31	17.21	0.11	0.03	17.24	**1.15**
	High	45.54	19.98	0.47	26.66	0.27	0.07	26.73	**0.75**
	Very High	46.41	20.36	0.84	47.11	0.52	0.14	47.25	**0.43**
Ensemble	Very Low	44.77	19.64	0.02	1.13	0.00	0.00	1.13	**17.39**
	Low	46.12	20.23	0.09	4.94	0.01	0.00	4.94	**4.10**
	Moderate	45.92	20.14	0.27	14.95	0.03	0.01	14.96	**1.35**
	High	44.91	19.70	0.37	20.87	0.19	0.05	20.93	**0.94**
	Very High	46.25	20.29	1.03	58.11	0.71	0.19	58.30	**0.35**

TABLE 6 Area under the curve (AUC) value of three models.

Models	Area	Standard error	Asymptotic significant	Asymptotic 95% confidence interval	
				Lower bound	Upper bound
Ensemble	**0.909**	0.008	0.000	0.893	0.925
EBF	**0.821**	0.011	0.000	0.799	0.844
LR	**0.802**	0.012	0.000	0.779	0.825

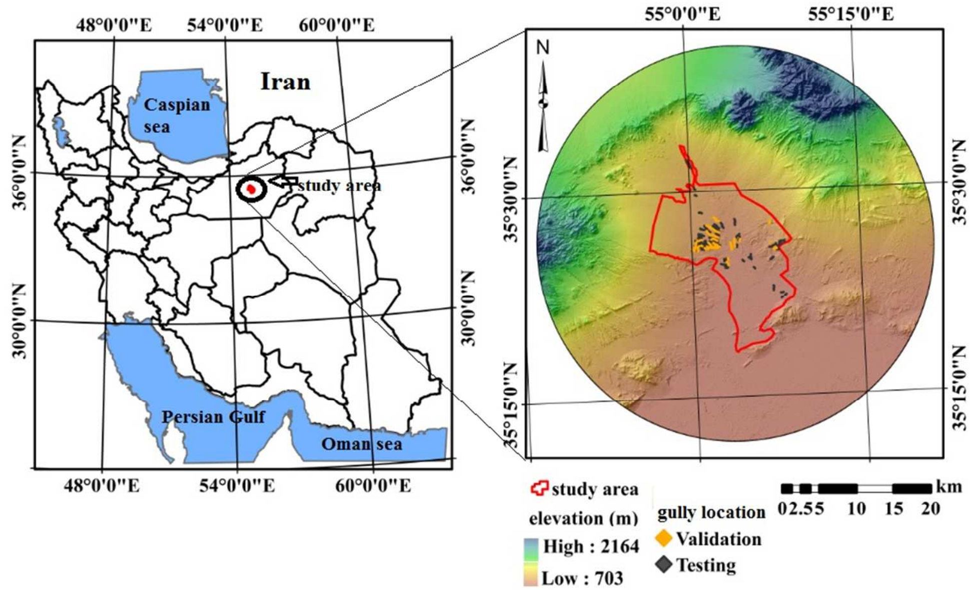

Fig. 1 Study area.

265x166mm (96 x 96 DPI)

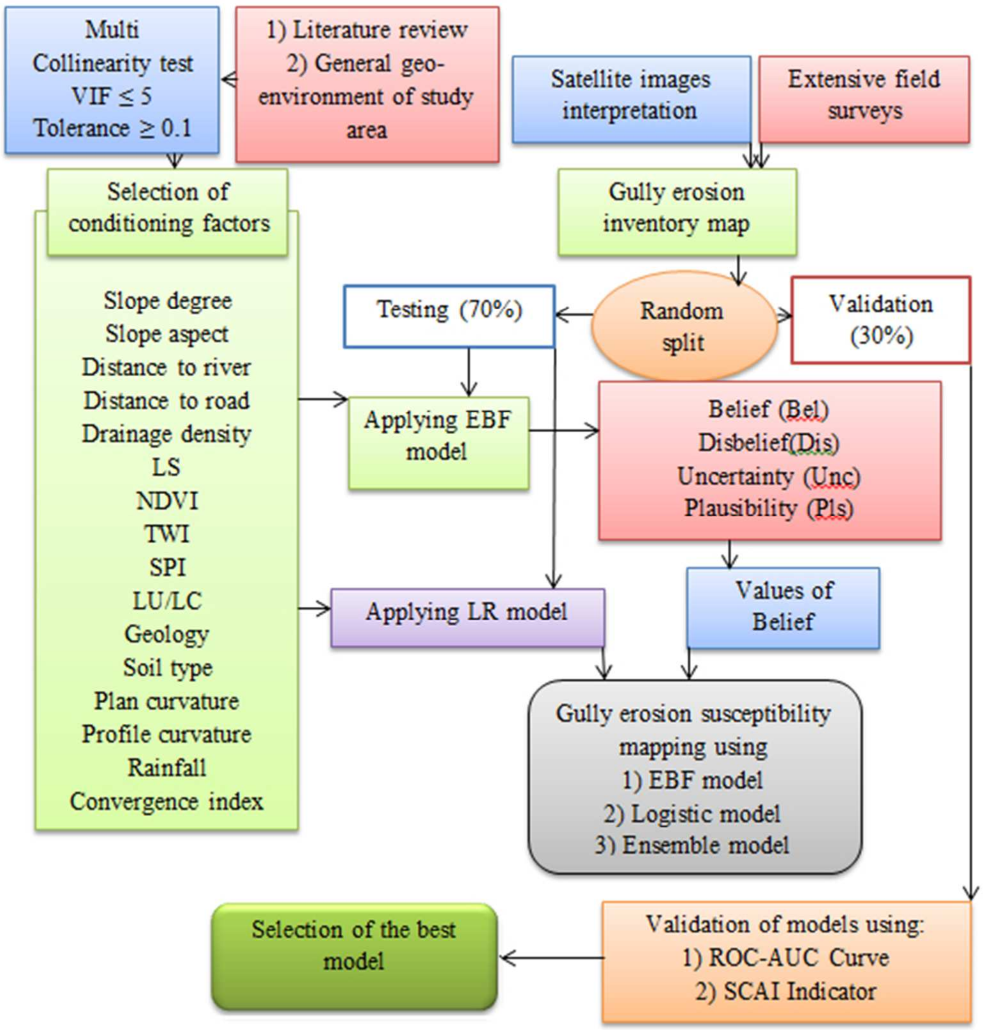

Fig. 2 Flowchart of the methodology used.

150x155mm (96 x 96 DPI)

Fig. 3 Field photographs showing identified gullies in the study area.

216x197mm (220 x 220 DPI)

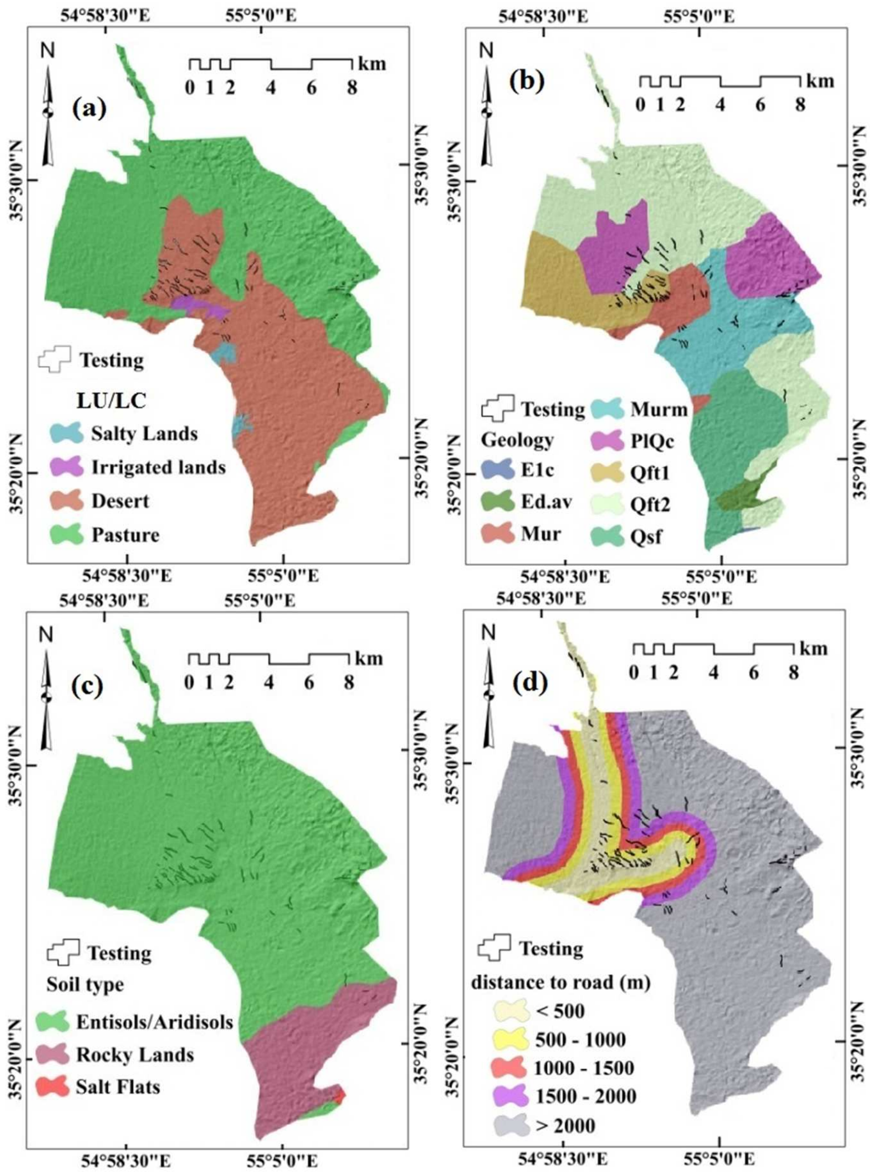

Fig. 4 Some examples of gully erosion conditioning factors, a) Land use/Land cover, b) lithology, c) soil type, and d) distance to road.

214x288mm (96 x 96 DPI)

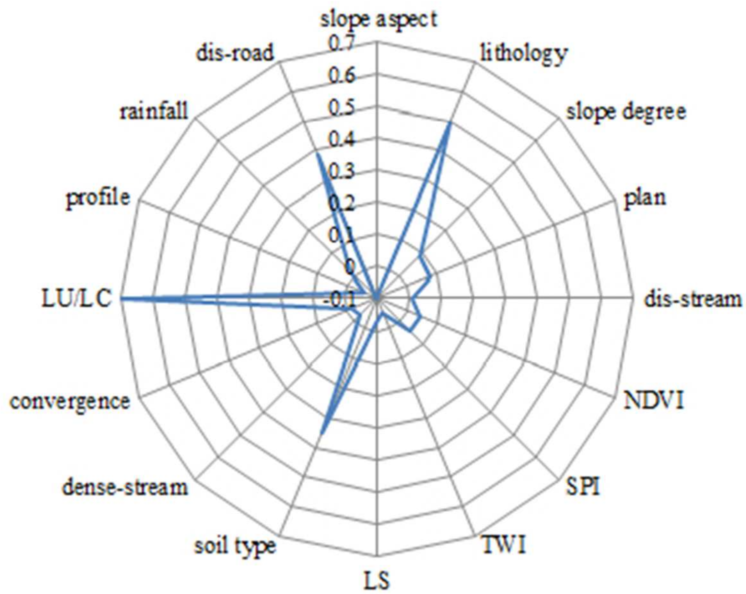

Fig. 5 Coefficients of conditioning factors in the logistic regression model.

101x79mm (96 x 96 DPI)

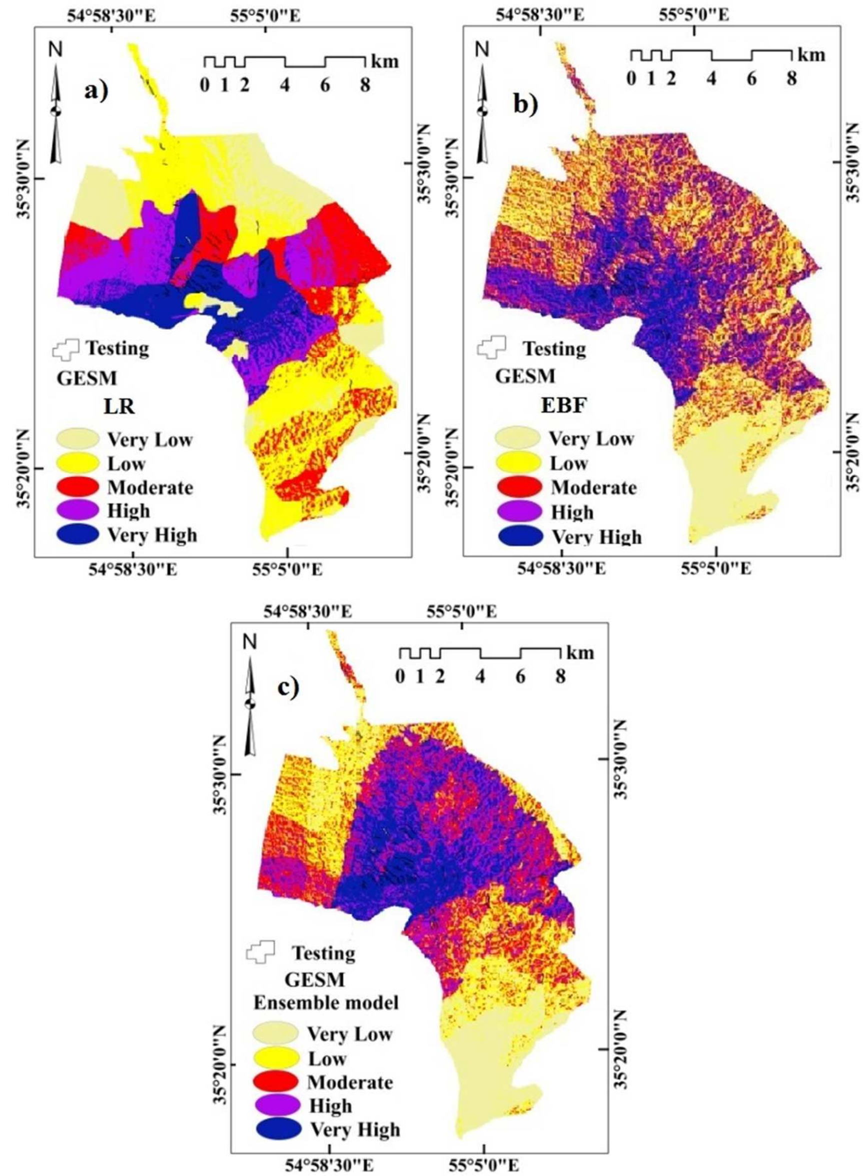

Fig. 6 Gully erosion susceptibility mapping using Logistic Regression (LR), Evidential Belief Function (EBF), and ensemble models.

212x292mm (96 x 96 DPI)